Journal of Sustainability for Energy
https://www.acadlore.com/journals/JSE

Enhancing Charge Transport and Stability in Perovskite Solar Cells via Integration with Porous Copper-Based Metal-Organic Frameworks

Muhammad Abid[1], Maryam Yasin[2], Muhammad Shahid[3], Saqib Murtaza[4*]

[1] Department of Mathematics, North Carolina State University, 27695 Raleigh, NC, United States
[2] Department of Physics, Faculty of Science, University of Agriculture, 38000 Faisalabad, Pakistan
[3] Department of Physics and Astronomy, Georgia State University, 30303 Atlanta, GA, USA
[4] Department of Mathematics, King Mongkut's University of Technology, 10140 Bangkok, Thailand

* Correspondence: Saqib Murtaza (saqib.murtaza@mail.kmutt.ac.th)

Received: 05-31-2024 **Revised:** 07-20-2024 **Accepted:** 07-29-2024

Citation: M. Abid, M.Yasin, M.Shahid, and S.Murtaza, "Enhancing charge transport and stability in perovskite solar cells via integration with porous copper-based metal-organic frameworks," *J. Sustain. Energy*, vol. 3, no. 3, pp. 139–153, 2024. https://doi.org/10.56578/jse030301.

Abstract: Perovskite solar cells (PSCs) have garnered significant attention in recent years due to their promising potential in photovoltaic applications. Ongoing research aims to enhance the efficiency, stability, and overall performance of PSCs. This study proposes the integration of copper-based metal-organic frameworks (Cu-MOFs) to address critical issues such as inadequate light absorption, instability, and suboptimal power conversion efficiency. Cu-MOFs, synthesized via the hydrothermal method at varying concentrations, have demonstrated an ability to mitigate defects in perovskite films and enhance charge transport. The structural versatility of Cu-MOFs allows for the development of new composites with improved stability and efficiency. By selecting the optimal MOF, hole transport layer (HTL), and counter-electrode materials, the performance of PSCs can be significantly improved. This research focuses on the functionalization of Cu-MOFs within PSCs to boost their efficiency. MOFs, which are porous materials composed of organic and inorganic components, are increasingly utilized in various fields including catalysis, energy storage, pollution treatment, and detection, due to their large surface area, tunable pore size, and adjustable pore volume. Despite their potential, the application of MOFs in aqueous environments has been limited by their poor performance. However, through techniques such as X-ray diffraction (XRD), UV-Vis spectroscopy, Raman spectroscopy, and scanning electron microscopy (SEM), it has been confirmed that Cu-MOFs can be successfully modified. Post-hydrothermal treatment, SEM results indicate enhanced stability and functionality of Cu-MOFs. The integration of Cu-MOFs in PSCs is expected to reduce energy consumption and significantly enhance the efficiency of these solar cells.

Keywords: Perovskite solar cells (PSCs); Copper-based metal-organic frameworks (Cu-MOFs); Charge transport layers; Optoelectronic properties; Stability and efficiency enhancement

1 Introduction

Nanoparticles are concerned with the fabrication, characterization, and use of substances and frameworks with dimensions that vary from 1 to 100 nm. The distinctive characteristics of nanomaterials make them valuable in a wide range of uses, such as solar cells, supercapacitors, and photocatalysis. By engineering the material at the nanoscale, the product's different macro- or micro-level attributes, including charge retention capacity, magnetism, and additional properties, are upgraded. Nanomaterials and devices improved by field research have numerous submissions and improved effectiveness [1]. Solar power is readily available and environmentally friendly, and it has the ability to end the current global shortage of energy. The primary type of energy that is renewable involves solar power due to its properties of zero pollution, resource independence, and economic viability. The largest source of clean energy is, without uncertainty, solar energy [2–4].

Solar cell concepts for the "next phase" were affordable and easy to make. Each of them stands for a newly created hybridized organometallic halogen perovskites-based solar panel, which gathered particular interest due to its highest recorded ease of production as well as affordability [5–7]. Third-generation solar cells made with silicon

have been dominant up to this point, with significant efficiency in converting power conversion efficiency (PCE) [8]. PSCs, a new third-generation solar cell type, provide a replacement for semiconductor solar cells that may have a PCE [9]. It has particular and good possibilities for development that are both functional and inexpensive [10]. This material refers to a class of compounds with the general crystal structure ABX3 (A and B are cations, while X is a halide or oxygen), which was first identified in 1839 by the Russian mineralogist L.A. Perovskite.

The structural and material instability of perovskite devices has a direct impact on how well they function. A large part of the inherent durability of perovskite materials is made up of moist strength, thermal properties, and transition persistence [11]. When exposed to brightness, each perovskite absorbance generates a particle of electrons that a hole forms as n-type as well as p-type carriers, which carry substances and generate charge-free agents. The mesoporous layer and external circuit were passed through by the produced electrons as they made their way to the cathode. As an outcome, the forced hole inside the HTM transmits in opposite directions between the sensors. In the end, it rearranges with an electron to form electricity. The current generation is affected by the size of the perovskite material [12]. Recent research concerning the possible usage of MOFs as PSCs that have been advertised as future solar cells capable of displacing conventional cells is summarized in detail [13].

MOFs, known as porous coordinated polymers (PCPs), can be utilized in a wide range of applications. This novel class of crystalline material is composed of coordination interactions and linking. Additionally, nano-MOFs with regulated shapes and sizes give an alternative option to traditional pristine MOFs. To create different nanostructures, MOFs are additionally used as support substrates for useful metals, metallic oxides, semiconductor products, and compounds used as sacrificial materials. MOFs with innovative structures and fascinating characteristics. Significant attempts have been undertaken to create MOFs [14, 15].

MOFs are increasing interest in some applications, including pollutant removal and senses, thanks to characteristics like wide surface area and variables that can increase pore size, quantity, and optimal function. Our objective for the article and the research referenced is to inspire researchers, especially material engineers, to examine [16]. Recently, the perovskite community has paid more attention to nanoscale Cu-MOFs because of their greatly improved PSC immovability and device performance, in addition to their wetness, chemical stability, and warm air stability.

Nanostructured Cu-MOFs that are both chemically and thermally stable are gaining a lot of attention as potential PSC materials. Cu-MOFs have been created using a lot of transition metal ions. Three sample-coordinating ligands are common materials containing carboxylate, phosphate, and carboxylate bonds in organic ligands. Their large range of coordinated numbers, states of oxidization, and topologies are mostly to blame for this. All of these techniques enhanced the Cu-MOF's thermodynamic stability, although their production is time-consuming [17]. Cu-MOF's hydrothermal stability may be improved through nanotube-containing silica; ceramics and the oxide of graphite have all been hybridized with various hydrophobic groups. In addition to being stable, Cu-MOFs can be treated in straightforward solutions. Their optoelectronic properties, allow for a variety of applications in PSCs. By enhancing the caliber of perovskite films, Cu-MOFs offer superior pathways and are efficient. We outline and discuss the many functions of Cu-MOFs in PSCs [18–21].

Low defect counts and high specific surface areas are key factors in enhancing PCE. Copper is a widely used n-type component as an ETL in PSCs because of its configurable electronic properties, adequate power level using perovskite, intrinsic openness, and low cost [22]. Cu features numerous defects, including metal interstitials with oxygen vacancies along contact and the borders of grains that are unfavorable for electron-collecting movement and result in high rates of photogenerated carrier recombination. Cu has poor conductivity and electron mobility [23]. To address this issue, some groups prepared porous Cu as ETL using Cu-MOF structures for MOF-based solar cells. A key advantage of the interaction of 3-dimensional (3D) perovskite formations with exceptionally porous Cu-MOF coats is their high stability, high carrier mobility, and large absorption coefficient [24, 25].

In conclusion, very few studies using metal oxide films have already been documented as utilized in PSCs thus far. Therefore, more research on Cu-MOF morphology regulation for improved PSC performance is needed. Due to their customizable architecture and configurable functions, MOFs have recently received more and more interest in PSC applications. However, Cu-MOF-modified HTL for PSC formation is still in its infancy. The primary research team concentrates on the alteration of HTL as a result of the inclusion of Cu-MOFs [26]. As a result, the development of HTM has a considerable influence on the PCEs and the long-term stability of PSCs [27]. A straightforward and step-by-step hydrothermal approach was used to create Cu-MOF to generate the HTL of PSCs. Due to the favorable energy levels of the perovskite and the HTL, increased HTL conductance and reduced defects in the outermost, and core-shell copper HTL were observed, primarily attributed to the efficient extraction of charge carriers [28].

A summary of current developments in a variety of MOFs, and their composites or derivatives have applications associated with energy is given in this paper. After that, we provide an update on the many uses for the energy of these materials, including fuel storage spaces, photo-induced creation of hydrogen, or greenhouse gas decrease, solar-powered battery cells, capacitors, lithium-based batteries, and water electrolysis. We start by outlining the components, structures, and unique properties of these substances as energy storage along with exchange. The discussion includes examples of solar usage utilizing MOFs, and their composites and derivatives.

2 Review of Literature

It explains that a cutting-edge application of nanotechnology is gaining more and more attention [29]. There are a lot of prospects in many different application domains thanks to the new deposition procedures that allow. In reaction to increased requirements for conservation of the environment and cleaner energy, the advancement of MOF thin film materials for application in solar energy systems, lowering CO_2 emissions, energy storage, splitting water into electrical devices, and fabrication of membranes has garnered an enormous amount of media coverage in recent years. The most recent developments in small films, such as production and patterning techniques, as well as current nanotechnology applications, were reviewed in this work. We end by outlining the most interesting potential prospects and pressing problems.

Describe that strong MOFs are porous materials formed by the interaction of metal ions with organic linkers [30]. MOFs have been used as precursors or sacrificing templates towards the development of a range of applications for functional nanostructures, in addition to their direct application. The current assessment covers the scientific literature on rechargeable batteries and batteries made of lithium-ion, electrocatalysts, catalysts for light, gas sensors, the processing of water and solar cells, and greenhouse gas removal. Finally, a future projection remains discussed, along with prospective opportunities for industrial applications [31].

At present, the photo transfer functionality of solar cells has increased. Metal batteries are popular because of their huge capacity, stable cycle achievement, low maintenance requirements, and flat charge possibility. Oxides and their composites (MOFs) are frequently investigated for use in PSCs [32]. Copper-based frameworks are a fantastic class of combined materials with pores that are currently generating a lot of interest [33]. Cu-MOFs were prospective candidates for medication delivery due to these properties. Cu-MOFs are a novel drug delivery system that demonstrates the efficiency of their use in the efficient delivery of numerous pharmaceuticals.

Additionally, researchers have also explored several strategies that can enhance the effectiveness of coverage. It had been employed regularly as a highly effective delivery system for pharmaceuticals to cancer cells. Finally, a thorough analysis of the issues and the potential for future development of MOFs incorporating copper as efficient drug release mechanisms was conducted. The Cu-MOFs-based medication delivery strategy had therefore enormous scientific value. The discussion below concentrates on the majority of modern uses of 3D Cu-MOF layouts in sectors that encompass metallurgy and related concerns such as drug administration, visualization, detection, and the preservation of hydrogen. Cu-MOFs had a variety of properties and qualities that had been modified, and those that had not been modified for usage in applications requiring controlled drug release were also discussed [34]. Metal-organic structures and compounds based on MOFs are popular because of their flexibility and strong catalytic capabilities are receiving increasing interest in precise chemical synthesis [35].

However, understanding the structure-reactivity relationship remains a major challenge to the further advancement of effective MOF-derived catalysts. The chemical makeup and physical characteristics of the MOF-derived support, among which are its area of surface, porosity, and metal species dispersion of variance, can be altered depending on the intended uses. As a result, MOF-derived materials provide a versatile framework allowing the development of effective accelerators in the manufacturing of micro molecules particularly associated stages. This presentation presented and reviewed a summary of advancements in the application of materials generated by MOFs in the manufacture of fine substances, and it also addressed a few crucial mediators [36].

Electrochemical synthesis: a few weeks ago, there had been quite an amount of fascination with cutting-edge [37]. The most popular techniques enabling the electrochemical creation of different MOFs on various bases, among other application advantages and disadvantages, were discussed in this chapter, along with how the attributes of the produced materials were modified by the chemical characteristics. Electrochemical techniques have been used to create many varieties of these coordination polymers. Electrochemical approaches offer some benefits over traditional MOF synthesis techniques, including quicker synthesis timeframes and the ability to adjust MOF. Changing the amount of electrical current or voltage changes the amount of thickness, shape, and milder synthesis conditions.

Modern photovoltaic cells are a crucial component of the continued development of environmentally acceptable solutions for everyday energy usage. Because of their outstanding compactness, greater electricity products or services, and guarantee of longer service cycles, batteries made of metal-air were establishing themselves as one of the most practical choices for storing solar energy [38]. Due to their diverse structural makeup, porosity benefits, tuneability, and high reactivity, functional materials produced from MOFs have found use as storage and conversion goods. In this paper, we provide a comprehensive overview of the most recent breakthroughs in MOF-based materials utilized in solar and metal-air battery applications [39].

Solvothermal production is a particularly efficient approach for producing MOFs, and it requires combining reactions such as ultrasonic stimulation, solvothermal process reaction, the output being washed, and solution drainage [40]. This approach allows for the production of homogeneous MOF microspheres with high phase uniformity and extremely small particle sizes, due to the rapid reaction kinetics of the solvothermal process. However, this method presents challenges during the washing process, which can lead to pore blockage if not adequately

managed. Insufficient removal of reacting substances can hinder the effectiveness of the MOF. Present-day research suggests incorporating centrifugal separations, considering optimum specifications at several independent levels: afterward reacting as well as after the result has been washed, enhance washing operations. The present effectiveness of CO_2 gas adsorption was used to access the average-level production process sample. The final sample of the optimized synthesis pathways had a CO_2 uptake capacity that was substantially greater compared to the example obtained from the fundamental combination and competitive with published data [41]. After centrifugation, the sample had a substantially greater crystallinity structure and was free of contaminants, according to analyses using a powder X-ray diffractometer (PXRD). Results suggested that washing operations successfully separated MOF products from reactive media, resulting in effective pore activation of MOFs [42].

Porous coordinating polymers and metal ions/clusters were used to create distinctive properties of MOFs, including structural diversity and tolerability. Their vast surface area, for example, makes them an extremely versatile platform for potential applications in a wide range of sectors [43]. This article discusses recent breakthroughs in MOF catalysis, such as heterogeneous catalysis, heterogeneous photosynthesis, and electricity production involving MOFs and MOF-based materials. The chemically active locations in the catalytic were given special attention. In terms of MOFs as well as associated elements for catalysis, difficulties, trends, and opportunities were also examined. MOFs that are hydrothermally stable are necessary for practical applications. Additionally, it was discovered that the degree of saturation in the parent MOF affects adsorption capability, selectivity, and hydrothermal stability [44].

3 Materials and Methods

3.1 Apparatus

Small beakers (50 ml), large beakers (100 ml), digital balance, magnetic stirrer, eppen drops, aluminum foil, centrifuge tubes, china dishes, electric oven, and furnace.

3.2 Chemicals

Copper sulphate pentahydrate $CuSO_4 \cdot 5H_2O$, carboxylic acid, methanol and distilled water.

3.2.1 Copper sulphate pentahydrate $CuSO_4 \cdot 5H_2O$

$CuSO_4 \cdot 5H_2O$ is the chemical formula for copper sulphate pentahydrate. It is a readily apparent homogeneous crystal that dissolves easily in water. It appears as a solid, brilliant blue color and we can see more in the Table 1. The average molecular weight is 249.65 g/mol. Copper sulphate pentahydrate has become a hydrated version of copper sulphate. Copper is a precious metal with excellent electrical and thermal conductivity as well as minimal oxidizing, alloying competence, and versatility.

Table 1. Copper sulphate pentahydrate properties

Property	Value
Chemical formula	$\mathrm{CuSO_4 \cdot 5H_2O}$
Molar mass	$249.68\ \mathrm{g/mol}$
Physical form	Powder
Melting point	$110^{\circ}\mathrm{C}$
Boiling point	$330^{\circ}\mathrm{C}$
Appearance	Blue crystals

3.2.2 Carboxylic acid

A carboxylic acid is an organic compound possessing a group that functions as a carboxyl. The most significant functioning group in C=O is the compound carboxylic acid. The general formula for carboxylic acid is R-COOH. Carboxylic compounds appear polarizing since they have the presence of these two electronegative oxygen atoms. The boiling point of a carboxylic acid is frequently higher than that of the same amount of water.

3.2.3 Methanol (CH_3OH)

Methanol (CH_3OH), often known as methyl alcohol, is the simplest and most basic of the many categories of chemical compounds. Pure methanol is a key component in chemical synthesis. Methanol is a transparent alcohol that melts at 64.96 degrees Celsius (148.93 degrees Fahrenheit) and freezes at 93.9 degrees Celsius (137 degrees Fahrenheit) chemicals and we can see more in the Table 2. The resulting compounds are widely employed in the production of a wide range of chemicals, including several important synthetic dyestuffs, resins, medicines, and perfumes.

Table 2. Properties of methanol (CH_3OH)

Sr	Chemical Formula	CH_3OH
1	Molar mass	$32.04\ \mathrm{g/mol}$
2	Boiling point	$64.7°\mathrm{C}$
3	Melting point	$-97.6°\mathrm{C}$
4	Density	$792\ \mathrm{kg/m^3}$
5	Classification	Chemical, Alcohol

3.2.4 Distilled water

Distilled water is water that has been purified through distillation, a process that separates pure $\mathrm{H_2O}$ from its impurities. It is produced by heating water until it vaporizes and then condensing the vapor back into liquid in a separate container. Pure distilled water should have a pH of 7, indicating that it is neutral.

3.3 Mathematical Configuration

The characterization and analysis of Cu-MOF and this thing integration into PSCs rely on particular fundamental mathematical equations for the establishment of this research method. These equations provide the basis for translating the experimental data and also for quantifying the accomplishments of the materials and devices. As the XRD analysis, a pivotal technique for identifying the crystal structure of Cu-MOF, is constructed based on the Bragg's Law:

$$n\lambda = 2d\sin\theta \tag{1}$$

where, n is an integer constituting the order of reflection, and also λ is the wavelength of the incident X-rays, moreover, d is the interplanar spacing in the crystal, and θ is the angle between the incident ray and the scattering planes. This equation authorizes the calculation of interplanar distances and also gives an advantage in identifying the crystal structure of the synthesized Cu-MOF. For the optical characterization by using the UV-visible spectroscopy, the Beer-Lambert Law is applied as follows:

$$A = \varepsilon bc \tag{2}$$

where, we have the absorbance as A, ε is the molar attenuation coefficient, b is the path length of the sample, and c is the concentration of the absorbing species. This particular equation is utilized to analyze the absorption spectra of Cu-MOF and also for estimate its optical properties, together with the band gap. The accomplishment of PSCs assimilating Cu-MOF is evaluated employing the PCE equation as follows:

$$PCE = \frac{V_{oc} * J_{sc} * FF}{P_{in}} \tag{3}$$

where, the open-circuit voltage is represented as V_{oc}, J_{sc} is the short-circuit current density, the fill factor is FF, and P_{in} is the incident light power. This equation provides a standardized measure for the solar cell's efficiency, allowing for comparison among the different device configurations as well as the materials.

These mathematical relationships form the strong foundation for the quantitative analysis of the properties of the Cu-MOF and also its influence on perovskite solar cell performance, authorizing an accurate evaluation of the material's potential in photovoltaic applications.

3.4 Experiment

For this paper, we performed the following experiments that are necessary for this research:

3.4.1 Synthesis of Cu-MOF

Pure Cu-MOF nanocrystals were created using the hydrothermal technique. In the present production, 2.2174g of $CuSO_4 \cdot 5H_2O$ was placed in 10ml of distilled water, then 1.05g equal carboxylic acid was dissolved in the provided solutions and magnetically stirred for 30 minutes at 80 °C to yield concentrations of 0.1M, 0.2M, and 0.3M. The reaction vessel was heated at 80 °C for three hours while being magnetically agitated. The product was collected by centrifugation at 6000 rpm and rinsed several times with distilled water. These solutions were then transferred to a one-hundred-milliliter Teflon-lined aluminum autoclave and deposited in a 120 °C oven for 12 hours for heat treatment. The solutions formed blue crystals, which were then filtered, rinsed using methanol and distilled water, and subsequently dried in a 145 °C furnace for 2 hours. The final step requires the resultant Cu-MOF to be washed with solvent to remove any unreacted components or impurities and then dried under vacuum or at low temperature (Figure 1).

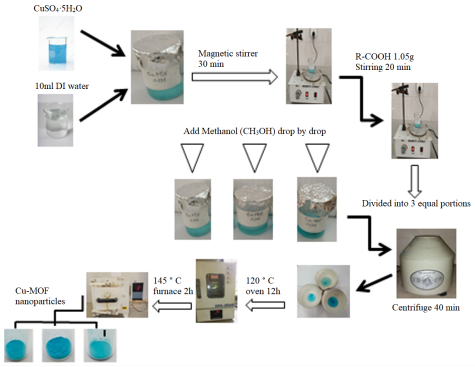

Figure 1. Preparation of Cu-MOF nanoparticles (0.1, 0.2, 0.3)

3.4.2 Characterization techniques

The crystalline process and phase purity of the synthesized Cu-MOF were examined using the PXRD technique. Also, the PXRD patterns were recorded in the 2θ using the range of 5-50° with a Bruker D8 Advance diffractometer with Cu Kα radiation ($\lambda = 1.5406°$A). The morphology and particle size of the Cu-MOF were identified by SEM using a JEOL JSM-7600F field emission SEM. So the optical properties, which also included absorption spectra and band gap estimation, were studied using a UV-Vis spectrophotometer (Shimadzu UV-2600) in the wavelength range of 200-800 nm.

3.4.3 Integration alongside PSCs

The synthesized Cu-MOF was integrated into the PSCs, either as an electron transport layer (ETL) or an HTL. In this regard, for ETL integration, a thin layer of Cu-MOF was deposited onto the fluorine-doped tin oxide (FTO) substrate, implementing spin-coating or doctor-blading techniques. The perovskite absorber layer was then integrated onto the Cu-MOF layer using a reasonable deposition method (e.g., the two-step sequential deposition, vacuum deposition, or vapor-assisted solution process). For the integration of HTL, the Cu-MOF layer was deposited onto the perovskite absorber layer, followed by the deposition of a metal back contact (e.g., gold, aluminum, or silver). The integration of Cu-MOF was anticipated to enhance charge transport and reduce defects in the perovskite absorber layer, leading to enhanced PCE and solar cell stability. The consequences of Cu-MOF incorporation on the photovoltaic performance of the devices were estimated by measuring the ongoing density-voltage (J-V) characteristics under the basic standard AM 1.5G illumination conditions.

3.4.4 Characterization of Cu-MOF-perovskite composites

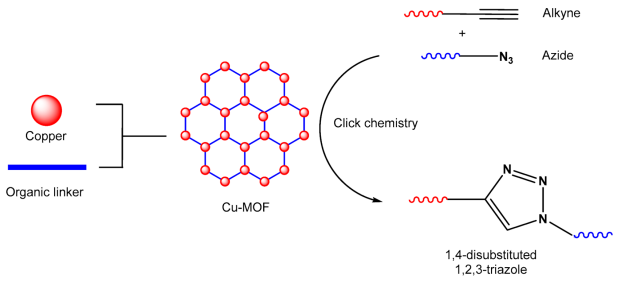

Figure 2. An illustration of MOF assembly and subsequent use in click chemistry

The morphological, structural, and optical properties of the Cu-MOF-perovskite composites were characterized using different techniques. The crystal structure and phase composition were examined by PXRD, and throughout the time, the surface morphology and elemental distribution were investigated by SEM and energy-dispersive X-ray spectroscopy (EDS). The optical properties, together with the absorption and photoluminescence spectra, were studied using UV-Vis and also with steady-state/time-resolved photoluminescence spectroscopy. So the charge transport as well as the recombination dynamics in the composites were examined by electrochemical impedance spectroscopy (EIS) and transient photovoltage/photocurrent measurements.

3.4.5 Stability and durability studies

The stability and durability of the Cu-MOF-PSCs in the long term were evaluated under different environmental conditions, including humidity, temperature, and light exposure. The devices were subjected to accelerated aging

tests, such as damp heat exposure (65°C, 85% relative humidity) and thermal cycling (-40°C to 85°C). The changes in photovoltaic performance and structural/morphological properties were monitored over time to assess stability and identify potential degradation mechanisms.

3.5 Physical Phenomena of Cu-MOF

To prepare for the ease of producing 1, 2, 3-triazole derivatives, the field of organic synthesis has worked intensively on developing innovative and effective Cu(I)-based MOF catalysts (Figure 2).

Cu-MOFs have grown in significance in the field of research due to their high catalytic capacity, plenty of assets, and easy synthesis, all of which are aided by copper's abundance in nature. Copper-containing catalysts offer a viable way for engaging initial components while maintaining reaction sensitivity under tunable circumstances, enabling the creation of complex frameworks from readily available building blocks (Figure 3). Cu(I) scaffolds encourage a variety of reaction methods, including CuAAC, oxidation, linking reactions, and Friedel-Craft acylation processes and can be seen in Figure 4. Adopted the hydrothermal synthesis of Cu-MOF, proposing an efficient but ecologically friendly way of synthesizing tetrazole derivatives utilizing Cu-MOF as a catalyst due to the extremely high crystallinity and purity of HKUST-1.

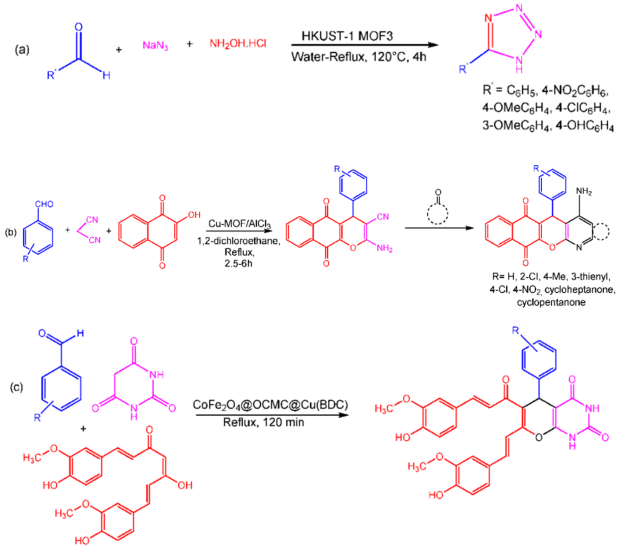

Figure 3. Different reactions catalyzed by Cu-MOFs (a) formation tetrazole from HKUST-1 MOF3 (b) three component coupling and cyclization reaction using Cu-MOF (c) single step three component coupling and cyclization reaction using CoFe2O4@OCMC@Cu(BDC)

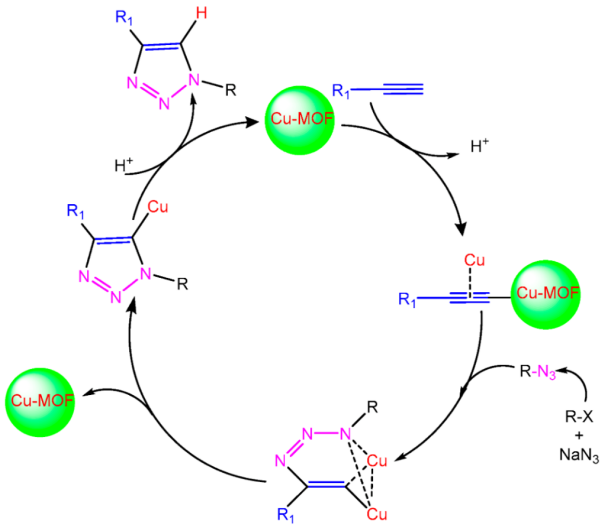

Figure 4. Plausible reaction mechanism for CuAAC using Cu-MOF as a catalyst

Sharpness, however, and colleagues proposed a chemical strategy for synthesizing 1, 4-disubstituted 1, 2, 3-triazoles utilizing a Cu alkynyl intermediate. But in addition to higher regioselectivity, a high yield and quick reaction kinetics are two of the most important advances observed by a number of scientists. Cu in the +1 oxidation state can be produced in situ using $CuSO_4 \cdot 5H_2O$ and sodium ascorbate or used directly as CuI, [Cu(PPh3)3Br], CuBr, Cu_2O, and other chemicals. Sharpless and colleagues first described a monofilament mechanism for the reaction's development; nevertheless, as scientific knowledge increased, Finn and Folkin identified and reported a binuclear process. In this method, two copper atoms link to the alkyne at distinct locations to create.

3.6 SEM

The scanning electron microscope, also known as SEM, is a type of microscopy that generates imaging using particles of electrons and not photons. The SEM has allowed researchers to examine a greater variety of specimens. A scanning electron microscope has an extensive depth of field, which allows more than one portion of a subject to become in focus at the same time. The SEM also has far higher resolution, which allows for considerably greater penetration of extremely close objects. When the electron beam interacts with the sample, it loses energy because of the spontaneous scattering as well as absorption by the substance.

3.7 XRD

It provides knowledge on the structure of crystal components, their sections, the crystallized initial phase, and additional properties. This is achieved using the XRD principle, whose effectiveness depends on the depth of X-ray beam transmission. The appearance of the diffraction pattern depends on the relative magnitude of the spectrum in relation to the measurements of the obstacle or opening it encounters. When a substance with a crystalline structure is analyzed, a three-dimensional pattern corresponding to the spacing of planes in the crystal lattice is generated, a phenomenon known as constructive interference.

3.8 UV-Visible Spectroscopy

UV-Vis spectroscopy (UV-Vis) is the study of absorption or reflectance during the ultraviolet-visible spectral range. Whenever something consumes ultraviolet (200-400 nanometers) to apparent (400-700 nanometers) radiation, the bonded as well as non-bonding electrons on the outside undergo a transition through the stationary configuration to the state of stimulation. This method makes use of the compound's capacity to absorb light at distinct wavelengths, which defines its absorption spectra. When favorable changes occur to determine the frequency range of light that is absorbed as well as the absorption peaks, which correspond with defining the sub-atomic structures, the UV-visible spectrum that characterizes a molecule offers knowledge regarding the ground state and what comes after the intermediate excited state.

4 Results and Discussion

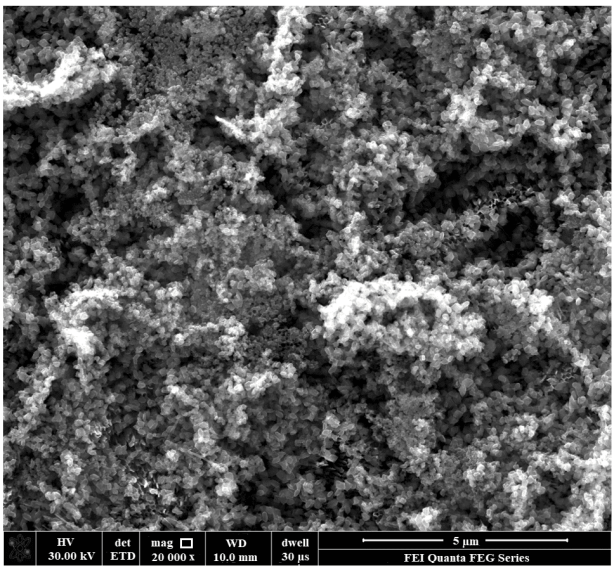

Figure 5. SEM image of Cu-MOF with $5\mu m$

Cu-MOF was synthesized at the University of Agriculture in Faisalabad, Pakistan, and characterized at the NUST (National University of Science and Technology) in Islamabad, Pakistan. SEM and XRD techniques will be utilized

to analyze Cu-MOF. The size of the crystal will be determined using XRD and a UV-Visible spectrometer will be required to examine absorption peaks and energy band gaps.

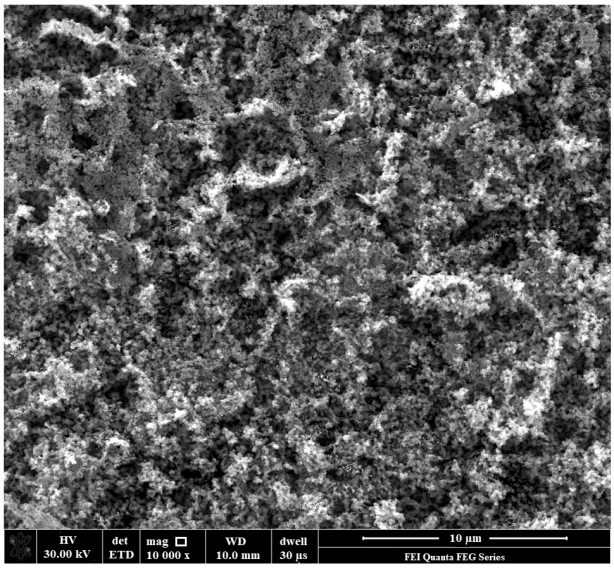

Figure 6. SEM image of Cu-MOF with $10\mu m$

4.1 Crystallinity Analysis

PXRD was used to evaluate the high crystallization while participating in the phasing purity of Cu-MOF. Aside from the underlying MOF peaks nationwide in the PXRD structure that modified Cu-MOF, the existence of PXRD peaks from the parent Cu-MOF, demonstrating that the MOF created was successfully functionalized. Extreme maxima at precise angles are characteristics that indicate microporous information, which contains countless microscopic openings or cavities. Peaks of functionalized diffraction are compared. Apart from having considerable amorphousness, specimens captured with parent Cu-MOF have very comparable diffraction patterns, demonstrating that the gemstone architecture associated with the MOF is generally preserved after functionalization. Nevertheless, after customization, the intensity of the Cu-MOF's major peak reflections decreased while the magnitude of the diffraction Bragg slope of some planes changed. These changes result from the pore-filling process that occurs in passageways in materials that are porous.

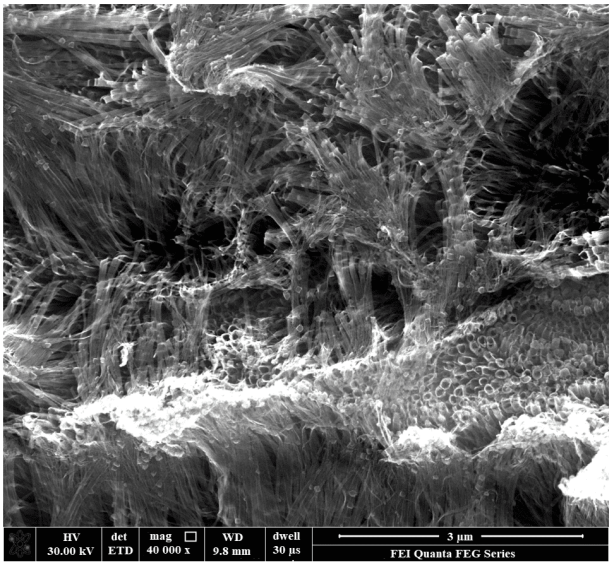

Figure 7. SEM images of synthesized Cu-MOFs after hydrothermal conditioning with $3\mu m$

4.2 Morphology of SEM

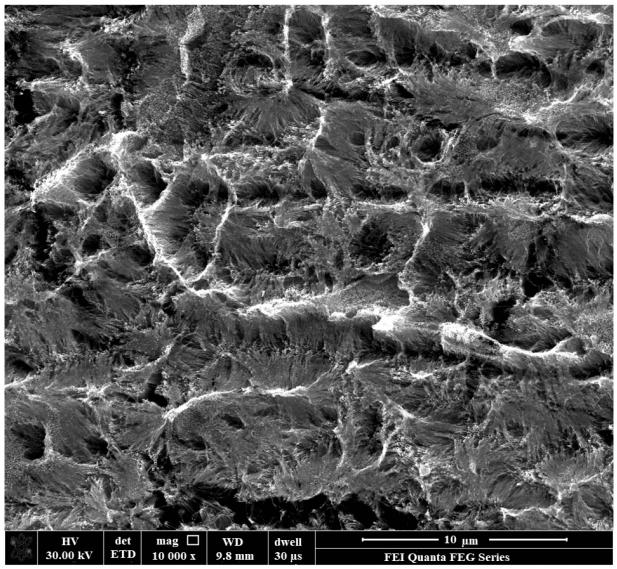

Figure 8. SEM images of synthesized Cu-MOFs after hydrothermal conditioning with 10μm

SEM is used in many different kinds of academic and commercial industries, including when solid particle characterization is important. A scanning electron microscope can observe and evaluate surface cracks, offer additional details in microstructures, start examining material contamination, demonstrate structural variations in elemental composition, offer additional qualitative synthetic studies, and describe the crystalline framework in addition to offering topographical, physical properties, and textual information. The exterior shape and elemental layout of Cu-MOF were investigated using SEM and EDS.

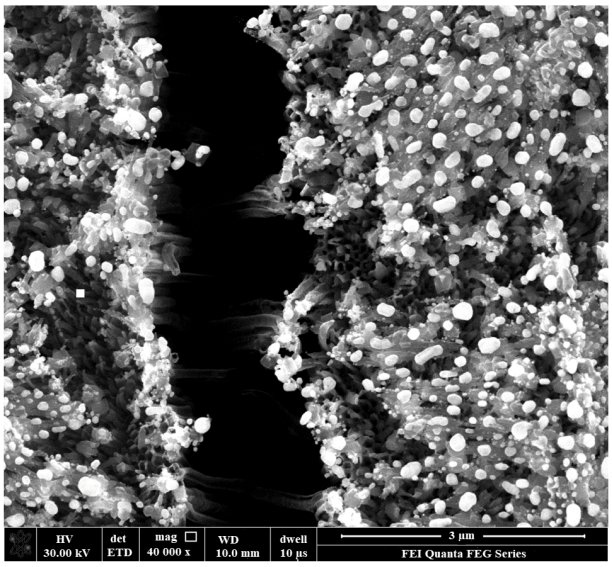

Figure 9. SEM images of synthesized Cu-MOFs after hydrothermal conditioning with 3μm

Figure 5 and Figure 6 demonstrate the morphologies of Cu-MOF films that are thin on an FTO substrate. The Cu-MOF film consists of spherical particles ranging in size from 02um to 500 nm (Figure 7).

The consistency of the Cu-MOF coating can be estimated from the SEM equipment's height profile module using the image evaluation technique, as illustrated in Figure 8, Figure 9, and Figure 10. The varied brightness on the topography SEM micrograph show the vertical height of the Cu-MOF coating.

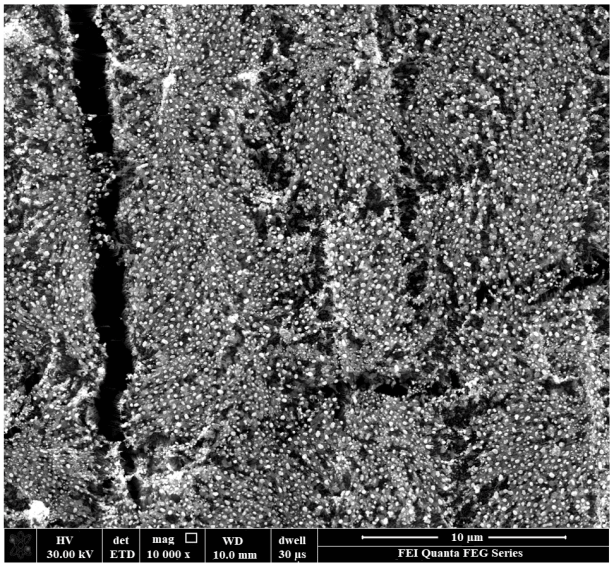

Figure 10. SEM images of synthesized Cu-MOFs after hydrothermal conditioning with $10\mu m$

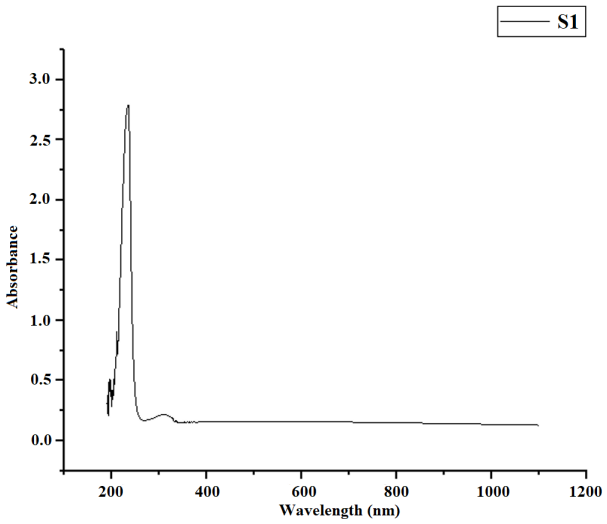

Figure 11. Thermal stability spectra Cu-MOF

4.3 Hydrothermal Conditioning

Considering high humidity and low-temperature circumstances, the intrinsic hydrodynamic behavior of basic Cu-MOFs versus enriched Cu-MOFs was investigated. All of the specimens ended up in the paper filter. They were placed in a container with water heated to approximately 85 degrees Celsius and left in the ambient water vapor for 5 hours. After hydrothermal conditioning, the samples were allowed to air out at room temperature, and images from the SEM were acquired to contrasting the structure within the collections before and following hydrothermal conditioning. The molecular structure of Cu-MOFs was well preserved throughout hydrothermal conditioning, as illustrated. However, the morphology of cleaner Cu-MOF as well as protein-enhanced Cu-MOF was substantially damaged. Cu-MOFs are stable, according to this study.

4.4 Thermal Stability Study

The produced samples are tested by exhausting thermo gravimetric exploration (TGA). TGA curves about the parent and functionalized Cu-MOFs. For synthesized Cu-MOF, two primary weight-decrease phases were found. First, the moisture in MOF was eliminated until it reached 130°C. After the solvent is removed, a steady upland appears. Temperatures up to 310°C have been recorded. The organic linker erosion caused a weight reduction, leading to the total implosion of the MOF structure. CuO powder was the leftover scrap. In all samples, with the stability of temperature of that pure Cu-MOF. The first water weight loss is substantially lower than the parent. As a

result, functionalized samples became more hydrophobic. Figure 11 indicates the thermal stability of a Cu-MOF.

The SEM photograph of HKUST-1 grains growing on the Cu-MOF material at ambient temperature with 200 spinning cycles is shown in Figure 12 and Figure 13. The dimensions of the sharp peak areas symbolize the average particle size, and the length of the variations and the separation in recurrent peaks or ridges represent the level of roughness and roughness width, respectively.

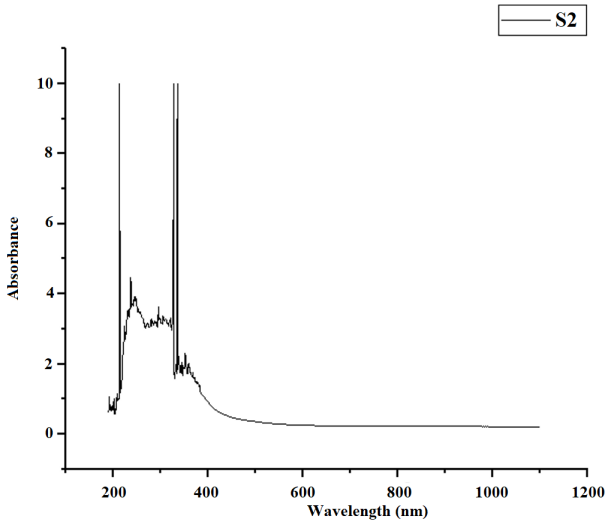

Figure 12. UV-Visible spectra of synthesized Cu-MOF

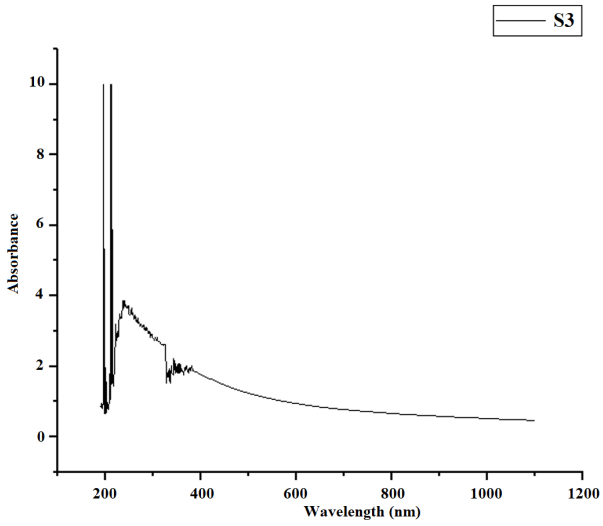

Figure 13. UV-Visible spectra Cu-MOF

5 Conclusion

The construction and modification of PSCs using Cu-MOF were described in the current article. Pre-functionalization of linkages usually causes issues in attaining desired results. MOFs were post-synthetically modified due to the unstable behavior of some functional groups in demanding MOF mixture settings, steric limitations produced by these molecules, and incursion throughout the crystallization procedure, which influences the porous nature of the MOF. Cu-MOF has been effectively functionalized with PSCs, as confirmed by SEM, Raman, and UV-Visible spectroscopy. XRD and SEM results confirmed the crystallinity and form of Cu-MOF. In SEM analysis, the initial step toward weight loss due to water evaporation in modified samples is significantly smaller than in the parent MOF, validating the concept of improved hydrothermal stability. Interaction measurements of angles and hydrothermal treatment methods provided additional support for the results presented. SEM data before and after hydrothermal conditioning showed that the modified samples performed best in terms of hydrothermal stability. The

thermodynamic stability of PSCs functionalized with Cu-MOF was determined using XRD, SEM, and UV-Visible spectroscopy. Additionally, the form and structure of the precursor Cu-MOF were influenced. According to their findings, the improved performance of PSCs functionalized with Cu-MOF holds great promise and serves various purposes such as monitoring, adsorption, and preservation.

6 Future Research Directions

Here are some potential future research directions for this current research project:

- Investigation of the electronic and optical properties of Cu-MOF: The paper briefly discusses the optoelectronic properties of Cu-MOF, but more comprehensive studies on the band gap, charge transport, and light absorption characteristics could provide valuable insights for their application in PSCs.
- Fabrication and testing of PSCs with Cu-MOF-based layers: The paper suggests the potential of using Cu-MOF as ETL, HTL, or interface modifiers in PSCs. Actual device fabrication and characterization under different operating conditions would be an important next step.
- Exploration of other transition metal-based MOFs for perovskite solar cell applications: The paper focuses on Cu-MOF, but investigating the performance of MOFs based on other transition metals, such as Fe, Co, or Ni, could lead to further improvements in perovskite solar cell efficiency and stability.
- Long-term stability studies of PSCs with Cu-MOF: Understanding the degradation mechanisms and developing strategies to improve the operational lifetime of PSCs incorporating Cu-MOF would be crucial for their practical implementation.
- Scale-up and cost analysis of Cu-MOF synthesis for commercial applications: Assessing the feasibility of large-scale production of Cu-MOF and evaluating the economic viability of using these materials in PSCs would be important for transitioning from lab-scale experiments to real-world applications.
- Exploration of other energy-related applications of Cu-MOF and its derivatives: The versatile nature of MOFs suggests that Cu-MOF and its functionalized forms could have potential applications in areas such as energy storage, catalysis, and gas separation, which could be further investigated.

Data Availability

The data used to support the findings of this study are available from the corresponding author upon request.

Conflicts of Interest

The authors declare that they have no conflicts of interest.

References

[1] G. Abdelmageed, L. Jewell, K. Hellier, L. Seymour, B. Luo, F. Bridges, J. Z. Zhang, and S. Carter, "Mechanisms for light induced degradation in $MAPbI_3$ perovskite thin films and solar cells," *Appl. Phys. Lett.*, vol. 109, no. 23, p. 233905, 2016. https://doi.org/10.1063/1.4967840

[2] M. Shen, Y. Zhang, H. Xu, and H. Ma, "MOFs based on the application and challenges of perovskite solar cells," *iScience*, vol. 24, no. 9, p. 103069, 2021. https://doi.org/10.1016/j.isci.2021.103069

[3] M. B. Tahir, S. Hajra, M. Rafique, and M. R. Hafeez, "Optical, microstructural and electrical studies on sol gel derived TiO_2 thin films," *Indian J. Pure Appl. Phys.*, vol. 55, no. 1, pp. 81–85, 2017.

[4] S. Chu and A. Majumdar, "Opportunities and challenges for a sustainable energy future," *Nature*, vol. 488, pp. 294–303, 2012. https://doi.org/10.1038/nature11475

[5] N. Rehman, M. Abid, and S. Qamar, "Numerical approximation of nonlinear and non-equilibrium model of gradient elution chromatography," *J. Liq. Chromatogr. Relat. Technol.*, vol. 44, no. 7-8, pp. 382–394, 2021. https://doi.org/10.1080/10826076.2021.1947316

[6] H. S. Jung and N. G. Park, "Perovskite solar cells: From materials to devices," *Small*, vol. 11, no. 1, pp. 10–25, 2015. https://doi.org/10.1002/smll.201402767

[7] N. J. Jeon, J. H. Noh, W. S. Yang, Y. C. Kim, S. Ryu, J. Seo, and S. I. Seok, "Compositional engineering of perovskite materials for high-performance solar cells," *Nature*, vol. 517, pp. 476–480, 2015. https://doi.org/10.1038/nature14133

[8] Meharunnisa, M. Saqlain, M. Abid, M. Awais, and Ž. Stević, "Analysis of software effort estimation by machine learning techniques," *Ing. Syst. Inf.*, vol. 28, no. 6, pp. 1445–1457, 2023. https://doi.org/10.18280/isi.280602

[9] C. Liu, J. Fan, H. Li, C. Zhang, and Y. Mai, "Highly efficient perovskite solar cells with substantial reduction of lead content," *Sci. Rep.*, vol. 6, no. 1, p. 35705, 2016. https://doi.org/10.1038/srep35705

[10] H. Furukawa, K. E. Cordova, M. O'Keeffe, and O. M. Yaghi, "The chemistry and applications of metal-organic frameworks," *Science*, vol. 341, no. 6149, p. 1230444, 2013. https://doi.org/10.1126/science.1230444

[11] K. Hindelang, A. Kronast, S. I. Vagin, and B. Rieger, "Functionalization of metal–organic frameworks through the postsynthetic transformation of olefin side groups," *Eur. J. Chem.*, vol. 19, no. 25, pp. 8244–8252, 2013. https://doi.org/10.1002/chem.201300477

[12] N. Singh and A. Thakur, "Applications of copper based metal organic frameworks," *Mater. Today: Proc.*, vol. 50, pp. 1906–1911, 2022. https://doi.org/10.1016/j.matpr.2021.09.264

[13] D. Y. Heo, H. H. Do, S. H. Ahn, and S. Y. Kim, "Metal-organic framework materials for perovskite solar cells," *Polymers*, vol. 12, no. 9, p. 2061, 2020. https://doi.org/10.3390/polym12092061

[14] A. G. Ahmad, M. K. Kaabar, S. Rashid, and M. Abid, "A novel numerical treatment of nonlinear and nonequilibrium model of gradient elution chromatography considering core-shell particles in the column," *Math. Probl. Eng.*, vol. 2022, no. 1, p. 1619702, 2022. https://doi.org/10.1155/2022/1619702

[15] L. Li, X. S. Wang, T. F. Liu, and J. Ye, "Titanium-based MOF materials: From crystal engineering to photocatalysis," *Small Methods*, vol. 4, no. 12, p. 2000486, 2020. https://doi.org/10.1002/smtd.202000486

[16] X. X. Feng, X. Lv, J. Cao, and Y. Tang, "Targeted management of perovskite film by Co (II) sulfophenyl porphyrin for efficient and stable solar cells," *Chin. J. Chem.*, vol. 41, no. 1, pp. 43–49, 2023. https://doi.org/10.1002/cjoc.202200468

[17] S. Akin, "Boosting the efficiency and stability of perovskite solar cells through facile molecular engineering approaches," *Sol. Energy*, vol. 199, pp. 136–142, 2020. https://doi.org/10.1016/j.solener.2020.02.025

[18] H. B. U. Haq, W. Akram, M. N. Irshad, A. Kosar, and M. Abid, "Enhanced real-time facial expression recognition using deep learning," *Acadlore Trans. Mach. Learn.*, vol. 3, no. 1, pp. 24–35, 2024. https://doi.org/10.56578/ataiml030103

[19] J. Liu and C. Wöll, "Surface-supported metal–organic framework thin films: Fabrication methods, applications, and challenges," *Chem. Soc. Rev.*, vol. 46, no. 19, pp. 5730–5770, 2017. https://doi.org/10.1039/C7CS00315C

[20] M. H. Yap, K. L. Fow, and G. Z. Chen, "Synthesis and applications of MOF-derived porous nanostructures," *Green Energy Environ.*, vol. 2, pp. 218–245, 2017. https://doi.org/10.1016/j.gee.2017.05.003

[21] F. Arjmand and Z. Rashidi Ranjbar, "Impact of copper and cobalt-based metal-organic framework materials on the performance and stability of hole-transfer layer (HTL)-free perovskite solar cells and carbon-based," *Sci. Rep.*, vol. 14, no. 1, p. 12843, 2024. https://doi.org/10.1038/s41598-024-62977-1

[22] M. Abid and M. Saqlain, "Decision-making for the bakery product transportation using linear programming," *Spectrum Eng. Manag. Sci.*, vol. 1, no. 1, pp. 1–12, 2023. https://doi.org/10.31181/sems1120235a

[23] H. Konnerth, B. M. Matsagar, S. S. Chen, M. H. Prechtl, F. K. Shieh, and K. C. W. Wu, "Metal-organic framework (MOF)-derived catalysts for fine chemical production," *Coord. Chem. Rev.*, vol. 416, p. 213319, 2020. https://doi.org/10.1016/j.ccr.2020.213319

[24] A. Ghoorchian, A. Afkhami, T. Madrakian, and M. Ahmadi, "Chapter 9 - Electrochemical synthesis of MOFs," in *Metal-Organic Frameworks for Biomedical Applications*, M. Mozafari, Ed. Woodhead Publishing, 2020, pp. 177–195. https://doi.org/10.1016/B978-0-12-816984-1.00011-1

[25] M. E. Hilal, A. Aboulouard, A. R. Akbar, H. A. Younus, N. Horzum, and F. Verpoort, "Progress of MOF-derived functional materials toward industrialization in solar cells and metal-air batteries," *Catalysts*, vol. 10, no. 8, p. 897, 2020. https://doi.org/10.3390/catal10080897

[26] K. Kamal, M. A. Bustam, M. Ismail, D. Grekov, A. Mohd Shariff, and P. Pré, "Optimization of washing processes in solvothermal synthesis of nickel-based MOF-74," *Materials*, vol. 13, no. 12, p. 2741, 2020. https://doi.org/10.3390/ma13122741

[27] L. Jiao, Y. Wang, H. L. Jiang, and Q. Xu, "Metal–organic frameworks as platforms for catalytic applications," *Adv. Mater.*, vol. 30, no. 37, p. 1703663, 2018. https://doi.org/10.1002/adma.201703663

[28] M. T. Hamid and M. Abid, "Decision support system for mobile phone selection utilizing fuzzy hypersoft sets and machine learning," *J. Intell. Manag. Decis.*, vol. 3, no. 2, pp. 104–115, 2024. https://doi.org/10.56578/jimd030204

[29] B. Singh and A. Indra, "Designing self-supported metal-organic framework derived catalysts for electrochemical water splitting," *Chem. Asian J.*, vol. 15, no. 6, pp. 607–623, 2020. https://doi.org/10.1002/asia.201901810

[30] M. Abid, N. Yasin, M. Saqlain, S. Ul-Islam, and S. Ahmad, "Numerical investigation and statistical analysis of the flow patterns behind square cylinders arranged in a staggered configuration utilizing the lattice Boltzmann method," *J. Appl. Fluid Mech.*, vol. 17, no. 9, pp. 1820–1843, 2024. https://doi.org/10.47176/jafm.17.9.2390

[31] M. W. Liu, G. Liu, Y. F. Wang, B. X. Lei, and W. Q. Wu, "Applications of multifunctional metal–organic frameworks in perovskite photovoltaics: Roles, advantages and prospects," *Mater. Chem. Front.*, vol. 8, no. 4, pp. 869–879, 2024. https://doi.org/10.1039/D3QM01001E

[32] M. Li, J. Wang, A. Jiang, D. Xia, X. Du, Y. Dong, P. Wang, R. Fan, and Y. Yang, "Metal organic framework doped Spiro-OMeTAD with increased conductivity for improving perovskite solar cell performance," *Sol.*

Energy, vol. 188, pp. 380–385, 2019. https://doi.org/10.1016/j.solener.2019.05.078

[33] A. M. Naji, S. H. Kareem, A. H. Faris, and M. K. Mohammed, "Polyaniline polymer-modified ZnO electron transport material for high-performance planar perovskite solar cells," *Ceram. Int.*, vol. 47, no. 23, pp. 33 390–33 397, 2021. https://doi.org/10.1016/j.ceramint.2021.08.244

[34] N. G. Park, "Perovskite solar cells: An emerging photovoltaic technology," *Mater. Today*, vol. 18, no. 2, pp. 65–72, 2015. https://doi.org/10.1016/j.mattod.2014.07.007

[35] F. Sadegh, S. Akin, M. Moghadam, V. Mirkhani, M. A. Ruiz-Preciado, Z. Wang, M. M. Tavakoli, M. Graetzel, A. Hagfeldt, and W. Tress, "Highly efficient, stable and hysteresis–less planar perovskite solar cell based on chemical bath treated Zn_2SnO_4 electron transport layer," *Nano Energy*, vol. 75, p. 105038, 2020. https://doi.org/10.1016/j.nanoen.2020.105038

[36] M. Abid and M. Saqlain, "Utilizing edge cloud computing and deep learning for enhanced risk assessment in China's international trade and investment," *Int. J. Knowl. Innov. Stud.*, vol. 1, no. 1, pp. 1–9, 2023. https://doi.org/10.56578/ijkis010101

[37] F. Hazeghi, S. Mozaffari, and S. M. B. Ghorashi, "Metal organic framework–derived core-shell CuO@NiO nanosphares as hole transport material in perovskite solar cell," *J. Solid State Electrochem.*, vol. 24, pp. 1427–1438, 2020. https://doi.org/10.1007/s10008-020-04643-w

[38] T. Zhang, F. Wang, H. B. Kim, and et al., "Ion-modulated radical doping of spiro-OMeTAD for more efficient and stable perovskite solar cells," *Science*, vol. 377, no. 6605, pp. 495–501, 2022. https://doi.org/10.1126/science.abo2757

[39] M. Abid, M. Bibi, N. Yasin, and M. Shahid, "A novel computational analysis of boundary driven two dimensional heat flow with the internal heat generation," *Comput. Algorithms Numer. Dimens.*, vol. 3, no. 1, pp. 1–16, 2024. https://doi.org/10.22105/cand.2024.443017.1090

[40] S. Zhang, F. Ye, X. Wang, and et al., "Minimizing buried interfacial defects for efficient inverted perovskite solar cells," *Science*, vol. 380, no. 6643, pp. 404–409, 2023. https://doi.org/10.1126/science.adg3755

[41] N. Al-Janabi, H. Deng, J. Borges, X. Liu, A. Garforth, F. R. Siperstein, and X. Fan, "A facile post-synthetic modification method to improve hydrothermal stability and CO_2 selectivity of CuBTC metal–organic framework," *Ind. Eng. Chem. Res.*, vol. 55, no. 29, pp. 7941–7949, 2016. https://doi.org/10.1021/acs.iecr.5b04217

[42] J. Feng, Y. Jiao, H. Wang, X. Zhu, Y. Sun, M. Du, Y. Cao, D. Yang, and S. Liu, "High-throughput large-area vacuum deposition for high-performance formamidine-based perovskite solar cells," *Energy Environ. Sci.*, vol. 14, no. 5, pp. 3035–3043, 2021. https://doi.org/10.1039/D1EE00634G

[43] S. Wang, L. Tan, J. Zhou, M. Li, X. Zhao, H. Li, W. Tress, L. Ding, M. Graetzel, and C. Yi, "Over 24% efficient MA-free $Cs_xFA_{1-x}PbX_3$ perovskite solar cells," *Joule*, vol. 6, no. 6, pp. 1344–1356, 2022. https://doi.org/10.1016/j.joule.2022.05.002

[44] S. Ahmad, "Vapor deposition as a promising approach for the large-scale perovskite solar cell fabrication," *iEnergy*, vol. 1, no. 2, p. 152, 2022. https://doi.org/10.23919/IEN.2022.0024